Understanding the history of complex ice crystal habits deduced from a holographic imager

J. T. Pasquier[1], J. Henneberger[1], A. Korolev[2], F. Ramelli[1], R. O. David[3], J. Wieder[1], A. Lauber[1,*], G. Li[1], T. Carlsen[3], R. Gierens[4], M. Maturilli[5], U. Lohmann[1]

[1]Institute for Atmospheric and Climate Science, ETH Zürich, Zurich, Switzerland
[2]Environment and Climate Change Canada, Toronto, Canada
[3]Department of Geosciences, University of Oslo, Oslo, Norway
[4]Institute for Geophysics and Meteorology, University of Cologne, Cologne, Germany
[5]Alfred Wegener Institute, Helmholtz Centre for Polar and Marine Research (AWI), Potsdam, Germany
*Now at: Center for Climate Systems Modelling (C2SM), ETH Zürich, Zurich, Switzerland

Key Points:

- A large variety of ice crystal sizes and shapes were observed in Arctic mixed-phase clouds with a holographic imager
- The growth history of two types of complex ice crystals was inferred from their shapes
- These ice crystals could enhance aggregation and secondary ice production

Corresponding author: J. T. Pasquier, julie.pasquier@env.ethz.ch

Corresponding author: J. Henneberger, jan.henneberger@env.ethz.ch

Abstract

The sizes and shapes of ice crystals influence the radiative properties of clouds, as well as precipitation initiation and aerosol scavenging. However, ice crystal growth mechanisms remain only partially characterized. We present the growth processes of two complex ice crystal habits observed in Arctic mixed-phase clouds during the NASCENT campaign. First, are capped-columns with multiple columns growing out of the plates' corners that we define as *columns on capped-columns* (CCC). These ice crystals originated from cycling through the columnar and plate temperature growth regimes, during their vertical transport by in-cloud circulation. Second, is aged rime on the surface of ice crystals having grown into faceted columns or plates depending on the environmental conditions. Despite their complexity, the shapes of these ice crystals allow to infer their growth history and provide information about the in-cloud conditions. Additionally, these ice crystals exhibit complex shapes and could enhance aggregation and secondary ice production.

Plain Language Summary

Snowflakes formed in the atmosphere have a wide variety of shapes and sizes and no two snowflakes are identical. The reason for this infinite number of shapes is that the environmental temperature and relative humidity prevailing during the snowflakes' growth determine their exact aspects. Thus, the shape of snowflakes provides information about the environmental conditions prevailing during their growth, but increasing shape complexity complicates the exact determination of the environmental conditions. During a measurement campaign in the Arctic, we identified two different complex types of snowflake and the history of environmental conditions in which they grew in. We inferred that some snowflakes were recirculating to higher or lower parts of the clouds and that other snowflakes had collided with cloud droplets that froze on their surface at the early stage of their growth. These snowflakes may further enhance the formation of new snowflakes and the initiation of precipitation.

1 Introduction

Clouds produce ice crystals of a fascinating diversity of shapes and patterns, and no two single ice crystals are identical (Bentley & Humphreys, 1931). The ice crystal shape influences the radiative properties of clouds (e.g., Yi et al., 2013; Järvinen et al., 2018)

as ice crystal habits influence their scattering properties (Wyser, 1999). In addition, the shapes and sizes of ice crystals determine their density, and therefore their fall velocities, which impacts their collision rates with other cloud particles. Furthermore, the ice crystal shape influences their interlocking and aggregation efficiencies (Connolly et al., 2012). The collision rate and aggregation efficiency of the ice crystals, in turn, determine precipitation formation. The shape, size, and fall velocity of ice crystals further affect their collision rates with aerosol particles and thus the scavenging rates, which influence the aerosol concentration and the aerosol radiative forcing (Croft et al., 2009). Thus, to understand the radiative properties of clouds, as well as precipitation initiation and aerosol scavenging, it is important to understand ice crystal growth mechanisms and to characterize ice crystal habits.

The exact shape of ice crystals grown by water vapor diffusion depends on the ambient temperature and water vapor supersaturation with respect to ice (Nakaya, 1954; Takahashi et al., 1991; Libbrecht, 2005). If the nucleation energy barrier for the basal face of the ice crystals is lower than that for the prism face, they grow faster toward the basal face and develop into plates (Libbrecht, 2005). In contrast, if the nucleation energy barrier for the prism face is lower than that of the basal face, the growth of the prism face is faster and the ice crystals develop into columns (Libbrecht, 2005). Nakaya (1954) investigated ice crystal shapes of precipitating snowflakes as well as synthetically grown ice crystals and summarized his observations into a so-called *snow crystal morphology diagram*. This diagram shows that the ice crystal's growth is plate-like at temperatures above -3°C, columnar between -3°C and -10°C, and plate-like again at colder temperatures. Furthermore, ice crystals exposed to higher supersaturation grow faster and develop into more complicated shapes, such as needles, sheaths (hollow columns or bullets), dendrites, and rosettes (Bailey & Hallett, 2009; Pruppacher & Klett, 2010; Knight, 2012), because the supersaturation and hence the crystal growth at tips and edges is faster than at a center of a face (Lamb & Verlinde, 2011). Thus, if ice crystals have a pristine shape, the temperature and supersaturation they experienced during growth by diffusion can be deduced, and the time of formation can be approximated from the size of the ice crystals. In other words, the appearance of ice crystals gives information about their history within clouds.

Subsequent to the work of Nakaya (1954), the growth of ice crystal was further studied and the ice crystal morphology diagram was improved. For instance (1) Kobayashi

(1958) studied the ice crystal growth as a function of pressure and described the growth of ice crystals at low water vapor saturation, (2) Kobayashi (1961), Takahashi et al. (1991) as well as Fukuta and Takahashi (1999) described the ice crystal growth under free fall in vertical supercooled cloud tunnels, (3) Bailey and Hallett (2004) and Bailey and Hallett (2009) improved the ice habit classification for temperature below -20°C using laboratory and field measurements, (4) Libbrecht (2005) and Libbrecht (2017) described with more precision the physical mechanisms governing the formation of ice crystals and grew ice crystals in controlled conditions in the laboratory. While Nakaya (1954) had already noted the presence of ice particles showing combinations of plate and columnar features in artificially grown ice crystals, Magono and Lee (1966) described in more detail the growth of ice crystals to plates and columns when growing in different environmental conditions and conceived an extensive table including these ice particles.

In addition to growth by diffusion, ice crystals can grow by aggregation with other ice crystals or by riming of cloud droplets on their surface, gradually losing their pristine original shapes. It is more difficult to determine the history of ice crystals with more complex shapes having grown by riming and aggregation.

Despite the extensive research performed over more than 90 years (e.g., Bentley & Humphreys, 1931; Nakaya, 1954; Korolev et al., 1999; Libbrecht, 2017), the ice crystal growth mechanisms remain only partially understood and characterized (Libbrecht, 2017). This work builds on previous studies investigating the growth history of ice crystals (e.g., Nakaya, 1954; Kobayashi, 1961; Magono & Lee, 1966; Libbrecht, 2005) and extends the analysis to two types of ice particles with complex habits.

2 Methods

The data presented in this paper was collected during the Ny-Ålesund AeroSol Cloud ExperimeNT (NASCENT) campaign, which took place from September 2019 to August 2020 in Ny-Ålesund, Svalbard (78.9°N, 11.9°E), and aimed at enhancing the knowledge about the chemical and microphysical properties of aerosols and clouds in the Arctic climate (Pasquier et al., 2022, accepted). In this study, the main instrument used is the HOLographic cloud Imager for Microscopic Objects (HOLIMO) that was mounted on the tethered balloon system HoloBalloon (Ramelli et al., 2020). HOLIMO uses holography to image cloud particles in the size range from small cloud droplets (6 µm) to large precipitating ice particles (2 mm) in a three-dimensional sample volume of approximately

15 cm^3 (Henneberger et al., 2013; Beck et al., 2017; Ramelli et al., 2020). Particles larger than 25 µm can be differentiated between cloud droplets and ice crystals based on their shapes (Henneberger et al., 2013). Ice crystals larger than 25 µm were identified with the help of a convolutional neural network trained and fine-tuned on cloud particles from holographic imagers (Touloupas et al., 2020; Lauber, 2020). Subsequently, the ice crystals were manually classified into habits according to their shape. In this study, we describe complex ice crystal habits observed on 11 November 2019 and 1 April 2020. A detailed description of the cloud microphysical properties and meteorological conditions on these days can be found in Pasquier et al. (2022).

The in-situ holographic measurements are complemented by ground-based remote sensing instruments installed at the French–German Arctic Research Base AWIPEV. In particular, the 94 GHz cloud radar of University of Cologne (JOYRAD-94, Küchler et al., 2017) is used to acquire continuous information on the vertical structure of the clouds. In this study, we use the measured Doppler velocity, which describes the sum of the updraft and radar reflectivity weighted fall velocities of cloud particles, as well as the reflectivity which is proportional to the sizes and concentrations of cloud particle. In addition, daily radiosonde launches (Maturilli & Kayser, 2017) provide information on the vertical distribution of wind, temperature, and humidity in the atmosphere.

3 Results

A large variety of ice crystal sizes and shapes were observed with HOLIMO during the NASCENT campaign. We identified three ice crystal shapes from the morphology diagram (Nakaya, 1954), i.e., columns, plates, and dendritic crystals (Fig. 1a-c). The columns had varying lengths (from a few micrometers to ∼1 cm) and varying aspect ratios (1 to 12) (Fig. 1a). Hollow columns were identified by their bright centers. The plates also ranged in a variety of sizes, thicknesses, and patterns (Fig. 1b). Finally, the presence of dendritic ice crystals was indicative of high supersaturation with respect to ice in the measured clouds (Fig. 1c). In addition to these pristine ice crystal habits, many irregular ice crystals with signs of aggregation and/or riming were observed (Fig. 1d). For these ice crystals, it is impossible to determine with certainty their underlying ice crystal habit(s) (e.g., column, plate, dendrite). Similar ice crystal habits have been reported in other Arctic mixed-phase clouds (e.g., Korolev et al., 1999; Lawson et al., 2001; McFarquhar et al., 2007; Avramov et al., 2011; Young et al., 2016; Mioche et al., 2017;

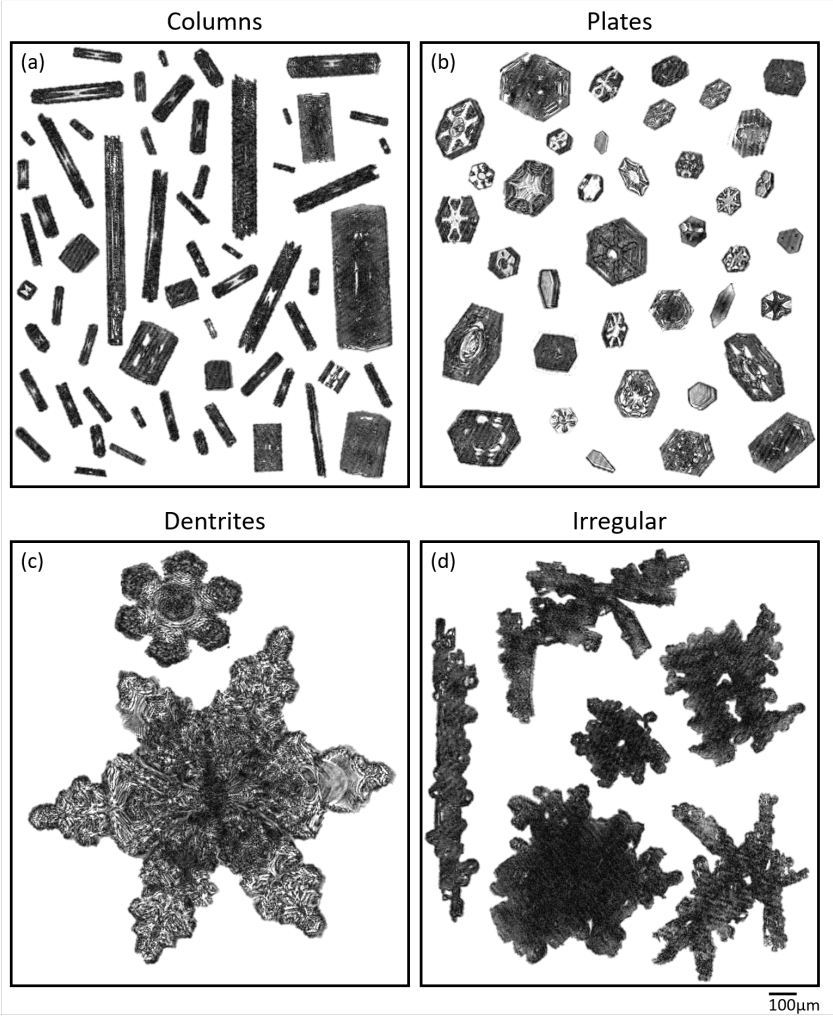

Figure 1. Examples of ice crystals observed with HOLIMO and classified manually as (a) columns, (b) plates, (c) dendrites, and (d) irregular ice particles. The scale bar at the bottom right applies for all panels.

Wendisch et al., 2019). Since these are common habits, they are not discussed further, but readers interested in a comprehensive description of the microphysical processes in these mixed-phase clouds are referred to Pasquier et al. (2022).

Additionally, we observed two distinguishable complex ice crystal habits for which it was possible to obtain information about their origin and growth history. First, ice particles with combinations of plates and columns were observed. These ice crystals were growing successively in different temperature regimes, which provides evidence for their recirculation within the clouds, and are named *columns on capped-columns* (CCC, Figs. 2, 3). Second, particles with faceted protuberances originating from growing rime that we

define as *aged rime particles* (Figs. 4,5). The collocation of in situ and remote sensing observations of thermodynamic and cloud microphysical variables allows for a detailed look into the growth processes of these two types of ice crystals in the following sections.

3.1 Observations of columns on capped-columns

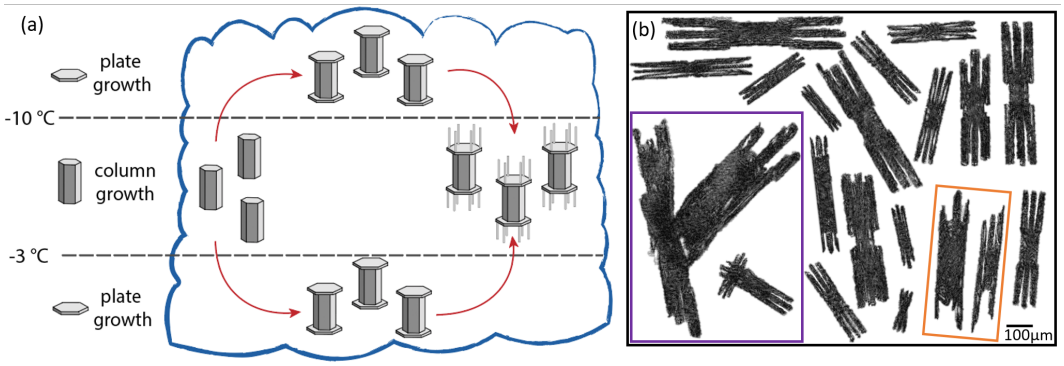

Figure 2. (a) Schematic of the growth of CCC particles through recirculation within clouds. (b) Examples of CCC particles observed with HOLIMO: two aggregated CCC particles are highlighted with the purple frame, CCC particles with a missing column are highlighted with the orange frame.

On 11 November 2019, HoloBalloon collected microphysical measurements in a stratocumulus cloud. The dominant ice crystal habits were columns, together with ice crystals showing signs of aggregation and riming (Pasquier et al., 2022). Additionally, capped-columns with multiple columns that grew from the corners of the plates were observed (Fig. 2b). We propose that these CCCs formed by undergoing the following process: ice particles first grew to columns, then plates formed at the basal planes of the column and the ice particles developed into capped-columns, and finally columns grew from the corners of the plates (Fig. 2a). This means that the CCC particles experienced successive growth in both the columnar (-3 °C < T < -10 °C) and plate (T > -3 °C or T < -10 °C) temperature regimes. A successive growth in the column - plate - column growth regimes was possible under the prevailing conditions in this cloud as the radiosonde launched at 20:00 UTC measured a temperature of -3°C at 300 m a.s.l., -10°C at 1300 m a.s.l., and -14°C at cloud top at 2200 m a.s.l. (Fig. 3). Additionally, the Doppler velocity indicated a turbulent cloud structure with rapidly changing updraft/downdraft regions within the cloud, enabling the lifting or falling of cloud particles (Fig. 3a). Finally, the high reflec-

tivity (> 0 dBZ) reaching up to 1500 m a.s.l. indicates the presence of larger ice crystals at this altitude (Fig. 3b).

We suggest that the CCCs started to grow as columns between -10°C and -3 °C at altitudes between 300 m a.s.l. and 1300 m a.s.l. (Fig. 2a). Then, they were transported either upward (above ∼ 1300 m a.s.l.) to colder (< -10°C) or downward (below ∼300 m a.s.l.) to warmer (> -3°C) regions of the cloud, where plate growth was favored, and developed into capped-columns (Fig. 2a). These crystals were then transported back to the columnar growth environment, and the columns grew out of the plate corners, where the water vapor supersaturation is highest (Fig. 2a). This was the only cloud case during the NASCENT campaign, where CCC particles were measured (likely due to the specific temperature/updraft combination necessary for their formation), but their concentration reached up to 17 L^{-1} which corresponds to 30% of the total ICNC at around 18:40 UTC (Fig. 3).

These CCC particles are not listed in the extensive morphology diagram developed by Magono and Lee (1966). To our knowledge, similar CCC particles were only observed in natural clouds by Libbrecht (2019) in Fairbanks, Alaska, and by Korolev et al. (2020) during a measurement flight in French Guiana. In both cases, the particles were observed at -5°C, which corresponds to the temperature range (-4°C to -5.5°C) at which we observed CCC particles on 11 November 2019 in Ny-Ålesund. In addition, similar particles could be formed in the laboratory, following temperature changes as discussed here (K. G. Libbrecht, personal communication).

Several measured CCC particles were aggregated (examples are shown with the purple frame in Fig. 2b). It was established that complex dendritic structures favor aggregation by improving mechanical interlocking (Barrett et al., 2019). As the CCC particles exhibit complex structures as well, they are likewise likely to favor aggregation. In addition, strong updrafts prevailed, enabling the lifting of ice particles within the cloud. Considerable lifting of ice particles likely increased the residence time of the ice particles in the cloud, allowing them to grow to larger size, and increasing the chance of collisions with other particles. The effect of the strong updraft together with complex structures of the CCC particles likely favored aggregation, which would have increased precipitation (Chellini et al., 2022).

Some particles were missing one or more columns growing from the plates (see particles highlighted with the orange frame in Figure 2b). As the outer columns of the CCC

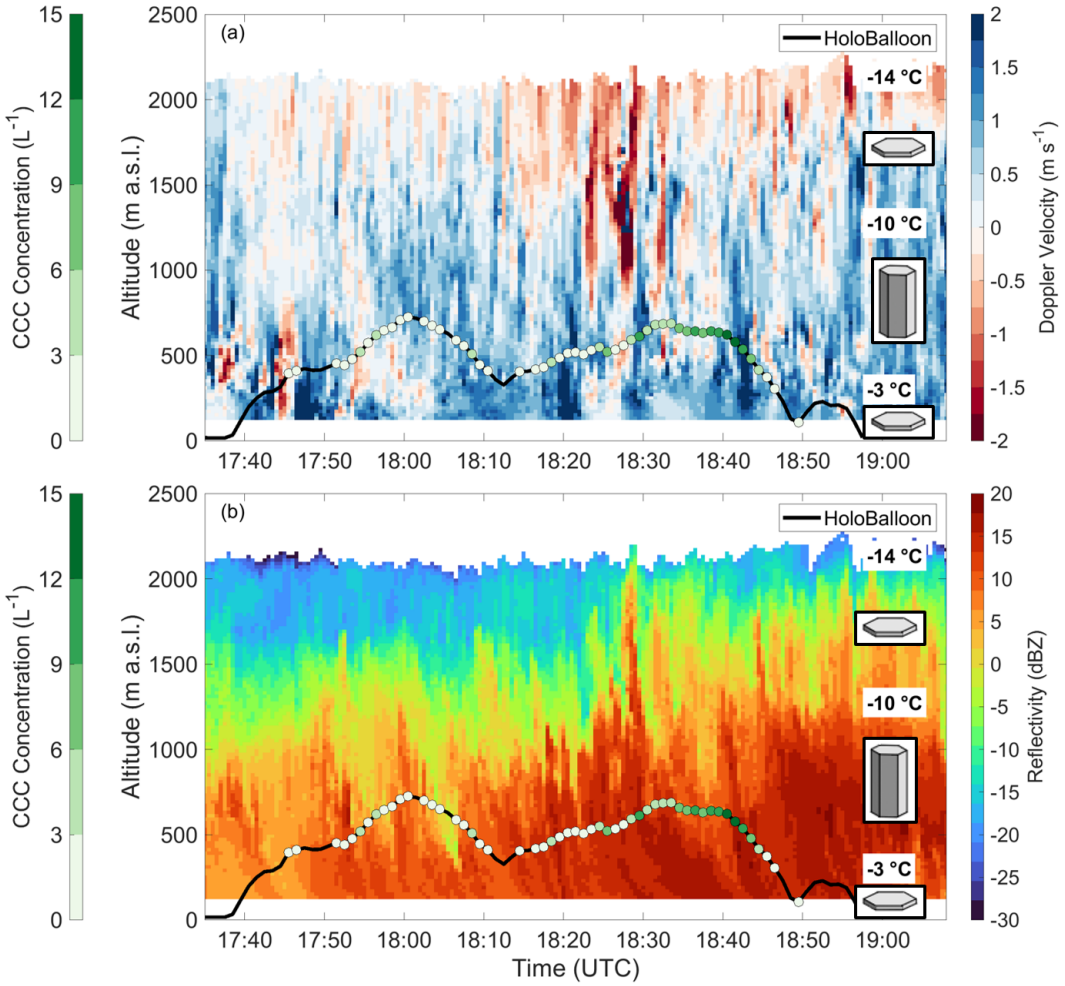

Figure 3. (a) Doppler velocity and (b) reflectivity measured by the cloud radar (color shading). HoloBalloon path (black line), and CCC concentration (dots, green shading) measured on 11 November 2019. The indicated temperatures were measured by a radiosonde launched at 20:00 UTC. Plate and column growth regions are illustrated with the respective symbols. Positive Doppler velocities correspond to downdrafts, and negative values correspond to updrafts in (a).

particles are rather fragile, it is possible that the branches broke off upon collision with other ice crystals, thereby creating secondary ice crystals. Indeed, secondary ice production was found to be enhanced between 18:20 UTC and 18:45 UTC on 11 November 2019, as described in Pasquier et al. (2022).

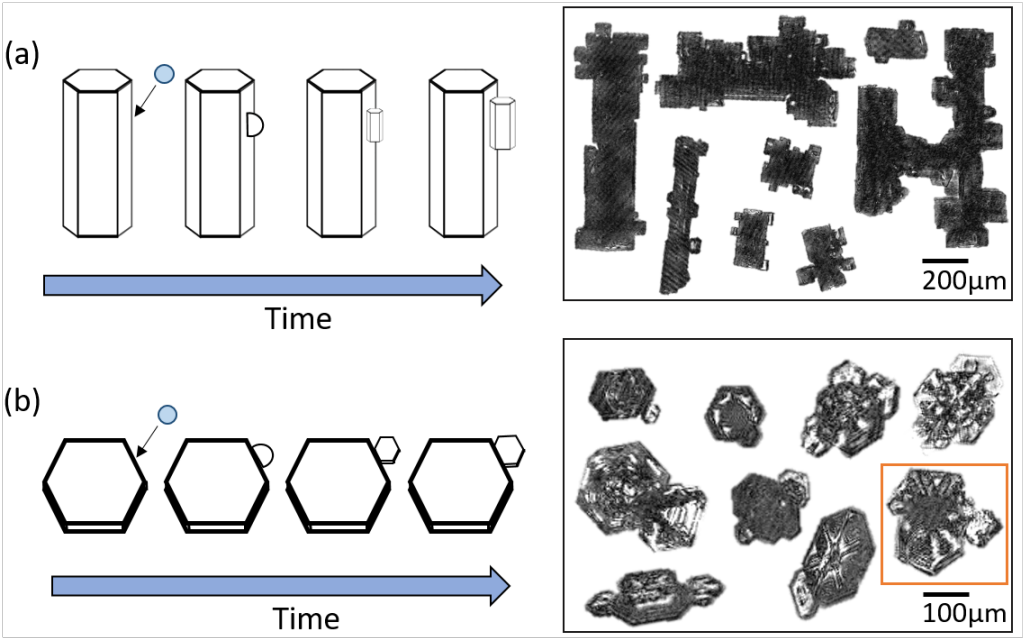

Figure 4. (a) Growth of columns and (b) plates after a cloud droplet collided, rimed, and grew in the columnar or plate regime. These ice crystals are termed aged rime particles, and examples of such ice crystals measured with HOLIMO are shown in the black frames on the right. An aged rime plate showing signs of breaking up is highlighted with an orange frame.

3.2 Observations of aged rime particles

Other ice crystals observed during the flight on 11 November 2019 with HOLIMO were aged rime columns. These particles have particular faceted protuberances that grew in the columnar growth regime, similar to the original column (Fig. 4a). Ice crystals showing similar, but plate-like, faceted protuberances growing on plates were observed on 1 April 2020 (Fig. 4b). On this day, the temperature in the cloud measured with HoloBalloon varied between -15°C to -23.5°C (Fig. 5), hence in the plate growth regime at low supersaturation with respect to ice (Nakaya, 1954). The increase in the radar reflectivity between 2000 m and 1000 m indicates that the layer was saturated with respect to ice. Moreover, the sharp increase in the radar reflectivity between 1200 m and 1000 m suggests the presence of an embedded supercooled liquid layer (Fig. 5b). Doppler velocities showed few variation except at around 14:30 UTC (Fig. 5a). We propose that the formation of aged rime ice crystals occurs as follows (Fig. 4): first cloud droplets rime on the columnar or plate-like ice crystal and freeze. The frozen protuberances then grow

on the basal face (plate growth regime) or prism face (columnar growth regime) depending on the temperature and supersaturation experienced. Note that the orientation of the growing protuberance in the basal or prism face remains identical to that of the original ice crystal (Pitter & Pruppacher, 1973; Iwabuchi & Magono, 1975; Uyeda & Kikuchi, 1978). This creates faceted protuberances observed on aged rime particles, compared to the smaller round protuberances observed on freshly rimed ice crystals. The presence of aged rime ice without fresh rime suggests that the ice crystal originates from a region with a higher liquid water content than at the measurement location and that they spent some time in the ice supersaturated, but liquid water subsaturated environment, sufficient to develop facets on the frozen droplets. As aged rime ice crystal concentrations up to 16 L^{-1} are measured during the HoloBalloon flight, we propose that the aged rime ice crystal experienced riming in the embedded supercooled liquid layer between 1000 m a.s.l. and 1200 m a.s.l. and grew to aged rime ice crystals during sedimentation to the altitude where they were observed with HoloBalloon.

The presence of rime growing to faceted protuberances was already mentioned for instance by Libbrecht (2005) for laboratory grown ice crystals and by Korolev et al. (2020) in natural clouds. Recently, Waitz et al. (2022) investigated riming in Arctic mixed-phase clouds and described similar aged rime particles as 'epitaxially' rimed in contrast to 'normal' rimed ice particles, the former most frequently prevailing in the temperature range between -10 °C and 0°C. It is interesting to note that aged rime ice crystals could be mistaken for aggregated particles due to their similar shapes. However, their formation arises from riming at an earlier stage of the growth process and not from aggregation with other ice crystals.

Several aged rime plates showed evidence of breaking up, as the particle highlighted with the orange frame in Figure 4b. The fragility of the aged rime plate particles could augment their chance of breaking up upon collision with other ice crystals. Therefore they could favor secondary ice production via the ice-ice collision process, as discussed in Pasquier et al. (2022).

4 Summary

The habits of pristine ice crystals can be used to identify their growth history within clouds, but determining the history of complex ice crystals that experienced aggregation or riming is difficult. Here, we present two types of complex ice crystal habits observed

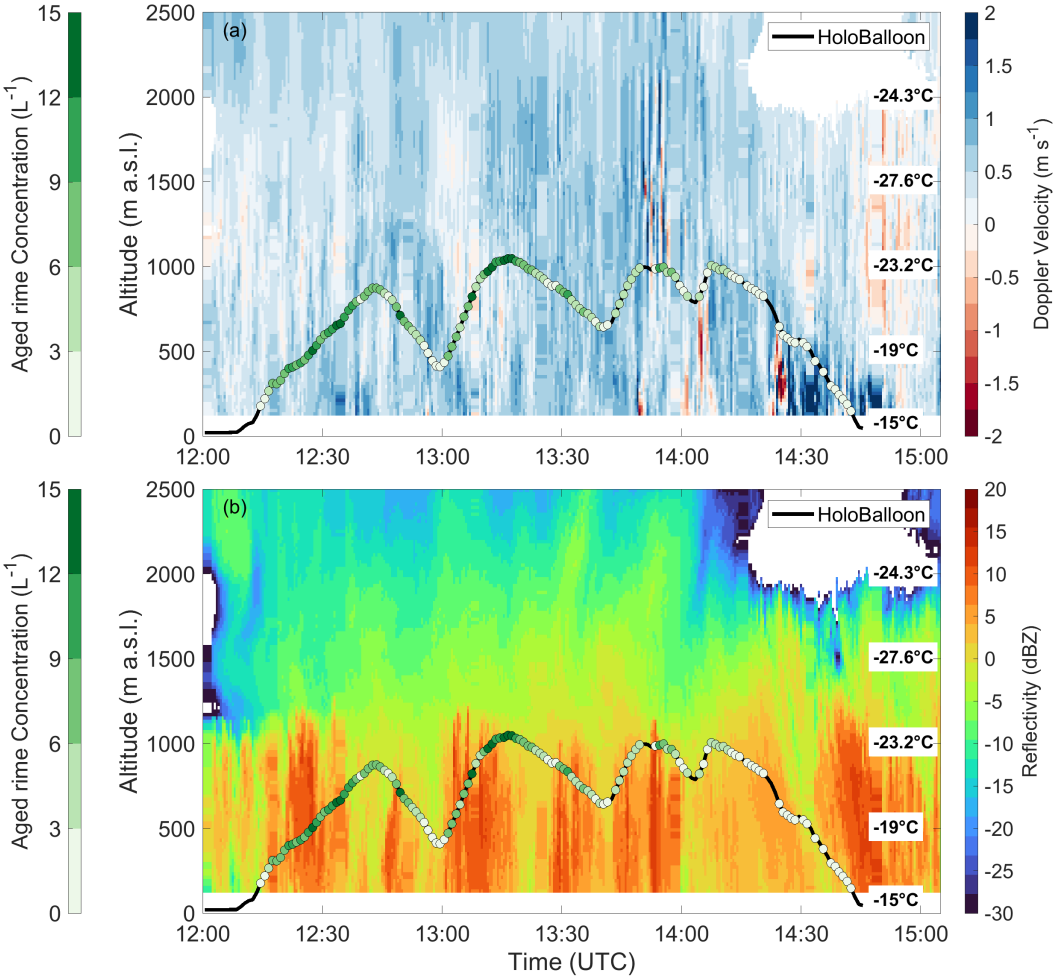

Figure 5. (a) Doppler velocity and (b) reflectivity measured by the cloud radar (color shading). HoloBalloon path (black line), and CCC concentration (dots, green shading) measured on 1 April 2020. The temperature is indicated every 500 m in altitude as measured by the radiosonde launched at 17:00 UTC.

in Arctic mixed-phase clouds during the NASCENT campaign, revealing their growth history despite their complex shapes.

First, the so-called columns on capped-columns (CCC) particles were growing successively in the column and plate growth regimes and exhibited a unique ice crystal shape corresponding to a capped-column with columns growing out of the corner of their plates (Fig. 2). Because the plate and column growth regimes are temperature constrained, we could determine that these ice crystals were recirculating between the upper and/or lower parts of the clouds where the temperature was below -10°C or above -3°C (plate growth regimes), and the column growth regime between -10°C and -3°C.

Second, aged rime plates and columns exhibiting faceted protuberances were observed, indicative of rime at the earlier stages of their growth process. After the rime froze on the surface of the plates and columns, it grew as a faceted protuberance with the same habit and along the same axis as the original ice crystal.

The observed CCC particles and aged rime ice crystals can influence the cloud microphysical properties, precipitation formation, and scavenging processes. For instance, CCC particles might favor aggregation by facilitating mechanical interlocking similarly to dendritical ice crystals (Barrett et al., 2019; Chellini et al., 2022), thereby enhancing precipitation and scavenging. Furthermore, observations of broken ice crystals suggest that both the outer columns of the CCC particles and the protuberances of the aged rime plates are fragile and thus could easily break off upon collision (Takahashi et al., 1995; Pasquier et al., 2022). Therefore, these ice crystals might favor secondary ice production via the ice-ice collision process.

5 Open Research

The cloud microphysical datasets as well as the scripts to reproduce the figures will be available on Zenodo (https://zenodo.org/). The radiosonde data are available in PANGAEA (`https://doi.pangaea.de/10.1594/PANGAEA.911039` & `https://doi.pangaea.de/10.1594/PANGAEA.917967`).

Acknowledgments

This project has received funding from the European Union's Horizon 2020 research and innovation programme under grant agreement No 821205 (FORCeS), from the Swiss Polar Institute (Exploratory Grants 2018), and from the Swiss National Science Foundation (SNSF) (grant No. 200021_175824). We gratefully acknowledge the funding by the European Research Council (ERC) through Grant StG758005. We would also like to acknowledge EEARO-NO-2019-0423/IceSafari, contract no. 31/2020, under the NO grants 2014–2021 of EEA Grants/Norway Grants for financial support. We gratefully acknowledge the funding by the Deutsche Forschungsgemeinschaft (DFG, German Research Foundation) – Project-ID 268020496 – TRR 172, within the Transregional Collaborative Research Center "ArctiC Amplification: Climate Relevant Atmospheric and SurfaCe Processes, and Feedback Mechanisms $(AC)^3$". We would also like to particularly thank Roland Neuber and Paul Zieger for their support and advice during the organisation of the campaign. The authors thank all those involved in the field work associated with NASCENT, particularly the AWIPEV and Norwegian Polar Institute Sverdrup stations staff.

References

Avramov, A., Ackerman, A. S., Fridlind, A. M., van Diedenhoven, B., Botta, G., Aydin, K., ... Wolde, M. (2011). Toward ice formation closure in arctic mixed-phase boundary layer clouds during isdac. *Journal of Geophysical Research: Atmospheres*, *116*(D1). Retrieved from https://agupubs.onlinelibrary.wiley.com/doi/abs/10.1029/2011JD015910 doi: https://doi.org/10.1029/2011JD015910

Bailey, M., & Hallett, J. (2004). Growth rates and habits of ice crystals between -20° and -70°c. *Journal of the Atmospheric Sciences*, *61*(5), 514 - 544. Retrieved from https://journals.ametsoc.org/view/journals/atsc/61/5/1520-0469_2004_061_0514_grahoi_2.0.co_2.xml doi: 10.1175/1520-0469(2004)061⟨0514:GRAHOI⟩2.0.CO;2

Bailey, M., & Hallett, J. (2009). A comprehensive habit diagram for atmospheric ice crystals: Confirmation from the laboratory, airs ii, and other field studies. *Journal of the Atmospheric Sciences*, *66*(9), 2888 - 2899. Retrieved from https://journals.ametsoc.org/view/journals/atsc/66/9/2009jas2883.1.xml doi: 10.1175/2009JAS2883.1

Barrett, A. I., Westbrook, C. D., Nicol, J. C., & Stein, T. H. M. (2019). Rapid ice aggregation process revealed through triple-wavelength doppler spectrum radar analysis. *Atmospheric Chemistry and Physics*, *19*(8), 5753–5769. Retrieved from https://acp.copernicus.org/articles/19/5753/2019/ doi: 10.5194/acp-19-5753-2019

Beck, A., Henneberger, J., Schöpfer, S., Fugal, J., & Lohmann, U. (2017). Hologondel: in situ cloud observations on a cable car in the Swiss Alps using a holographic imager. *Atmospheric Measurement Techniques*, *10*(2), 459–476. doi: 10.5194/amt-10-459-2017

Bentley, W., & Humphreys, W. (1931). Snow crystals, mcgraw-hili book company. *Inc., 226pp*.

Chellini, G., Gierens, R., & Kneifel, S. (2022). Ice aggregation in arctic shallow mixed-phase clouds: enhanced by dendritic growth and absent close to the melting level. *Earth and Space Science Open Archive*, 32. Retrieved from https://doi.org/10.1002/essoar.10511005.1 doi: 10.1002/essoar.10511005.1

Connolly, P. J., Emersic, C., & Field, P. R. (2012). A laboratory investigation into the aggregation efficiency of small ice crystals. *Atmospheric Chemistry and Physics*, *12*(4), 2055–2076. Retrieved from https://acp.copernicus.org/articles/12/2055/2012/ doi: 10.5194/acp-12-2055-2012

Croft, B., Lohmann, U., Martin, R. V., Stier, P., Wurzler, S., Feichter, J., ... Ferrachat, S. (2009). Aerosol size-dependent below-cloud scavenging by rain and snow in the echam5-ham. *Atmospheric Chemistry and Physics*, *9*(14), 4653–4675. Retrieved from https://acp.copernicus.org/articles/9/4653/2009/ doi: 10.5194/acp-9-4653-2009

Fukuta, N., & Takahashi, T. (1999, 06). The Growth of Atmospheric Ice Crystals: A Summary of Findings in Vertical Supercooled Cloud Tunnel Studies. *Journal of the Atmospheric Sciences*, *56*(12), 1963-1979. doi: 10.1175/1520-0469(1999)056⟨1963:TGOAIC⟩2.0.CO;2

Henneberger, J., Fugal, J. P., Stetzer, O., & Lohmann, U. (2013). HOLIMO II: a digital holographic instrument for ground-based in situ observations of microphysical properties of mixed-phase clouds. *Atmospheric Measurement Techniques*, *6*(11), 2975–2987. doi: 10.5194/amt-6-2975-2013

Iwabuchi, T., & Magono, C. (1975). A laboratory experiment on the freezing electrification of freely falling water droplets. *Journal of the Meteorological Society of Japan. Ser. II*, *53*(6), 393-401. doi: 10.2151/jmsj1965.53.6_393

Järvinen, E., Jourdan, O., Neubauer, D., Yao, B., Liu, C., Andreae, M. O., ... Schnaiter, M. (2018). Additional global climate cooling by clouds due to ice crystal complexity. *Atmospheric Chemistry and Physics*, *18*(21), 15767–15781. Retrieved from https://acp.copernicus.org/articles/18/15767/2018/ doi: 10.5194/acp-18-15767-2018

Knight, C. A. (2012). Ice growth from the vapor at -5°c. *Journal of the Atmospheric Sciences*, *69*(6), 2031 - 2040. Retrieved from https://journals.ametsoc.org/view/journals/atsc/69/6/jas-d-11-0287.1.xml doi: 10.1175/JAS-D-11-0287.1

Kobayashi, T. (1958). On the habit of snow crystals artificially produced at low pressures. *Journal of the Meteorological Society of Japan. Ser. II*, *36*(5), 193-208. doi: 10.2151/jmsj1923.36.5_193

Kobayashi, T. (1961). The growth of snow crystals at low supersaturations. *The*

Philosophical Magazine: A Journal of Theoretical Experimental and Applied Physics, *6*(71), 1363-1370. Retrieved from https://doi.org/10.1080/14786436108241231 doi: 10.1080/14786436108241231

Korolev, A., Heckman, I., Wolde, M., Ackerman, A. S., Fridlind, A. M., Ladino, L. A., ... Williams, E. (2020). A new look at the environmental conditions favorable to secondary ice production. *Atmospheric Chemistry and Physics*, *20*(3), 1391–1429. doi: 10.5194/acp-20-1391-2020

Korolev, A., Isaac, G. A., & Hallett, J. (1999). Ice particle habits in arctic clouds. *Geophysical Research Letters*, *26*(9), 1299-1302. Retrieved from https://agupubs.onlinelibrary.wiley.com/doi/abs/10.1029/1999GL900232 doi: https://doi.org/10.1029/1999GL900232

Küchler, N., Kneifel, S., Löhnert, U., Kollias, P., Czekala, H., & Rose, T. (2017). A W-Band Radar-Radiometer System for Accurate and Continuous Monitoring of Clouds and Precipitation. , *34*, 2375-2392. doi: 10.1175/JTECH-D-17-0019.1

Lamb, D., & Verlinde, J. (2011). *Physics and chemistry of clouds.* Cambridge University Press.

Lauber, A. (2020). *In-situ observations of ice multiplication in clouds using a holographic imager and a deep learning algorithm for the classification of cloud particles* (Doctoral dissertation, ETH Zurich, Zurich). doi: 10.3929/ethz-b-000474830

Lawson, R. P., Baker, B. A., Schmitt, C. G., & Jensen, T. L. (2001). An overview of microphysical properties of Arctic clouds observed in May and July 1998 during FIRE ACE. *Journal of Geophysical Research: Atmospheres*, *106*(D14), 14989-15014. doi: 10.1029/2000JD900789

Libbrecht, K. G. (2005, mar). The physics of snow crystals. *Reports on Progress in Physics*, *68*(4), 855–895. doi: 10.1088/0034-4885/68/4/r03

Libbrecht, K. G. (2017). Physical dynamics of ice crystal growth. *Annual Review of Materials Research*, *47*(1), 271-295. Retrieved from https://doi.org/10.1146/annurev-matsci-070616-124135 doi: 10.1146/annurev-matsci-070616-124135

Libbrecht, K. G. (2019). *Snow crystals.* arXiv. Retrieved from https://arxiv.org/abs/1910.06389 doi: 10.48550/ARXIV.1910.06389

Magono, C., & Lee, C. W. (1966). Meteorological classification of natural snow crystals. *Journal of the Faculty of Science, Hokkaido University. Series 7, Geophysics*, *2*(4), 321–335.

Maturilli, M., & Kayser, K. (2017). Arctic warming, moisture increase and circulation changes observed in the Ny-Ålesund homogenized radiosonde record. *Theoretical and Applied Climatology*, *130*(1-17), 1434-4483. doi: 10.1007/s00704-016-1864-0

McFarquhar, G. M., Zhang, G., Poellot, M. R., Kok, G. L., McCoy, R., Tooman, T., ... Heymsfield, A. J. (2007). Ice properties of single-layer stratocumulus during the mixed-phase arctic cloud experiment: 1. observations. *Journal of Geophysical Research: Atmospheres*, *112*(D24). Retrieved from https://agupubs.onlinelibrary.wiley.com/doi/abs/10.1029/2007JD008633 doi: https://doi.org/10.1029/2007JD008633

Mioche, G., Jourdan, O., Delanoë, J., Gourbeyre, C., Febvre, G., Dupuy, R., ... Gayet, J.-F. (2017). Vertical distribution of microphysical properties of arctic springtime low-level mixed-phase clouds over the greenland and norwegian seas. *Atmospheric Chemistry and Physics*, *17*(20), 12845–12869. Retrieved from https://acp.copernicus.org/articles/17/12845/2017/ doi: 10.5194/acp-17-12845-2017

Nakaya, U. (1954). *Snow crystals: Natural and artificial*. Cambridge, MA: Harvard University Press.

Pasquier, J. T., David, R. O., Freitas, G., Gierens, R., Gramlich, Y., & Haslett, e. a., S. (2022, accepted). The ny-Ålesund aerosol cloud experiment (nascent): Overview and first results. *Bulletin of the American Meteorological Society*.

Pasquier, J. T., Henneberger, J., Ramelli, F., Lauber, A., David, R. O., Wieder, J., ... Lohmann, U. (2022). Conditions favorable for secondary ice production in arctic mixed-phase clouds. *Atmospheric Chemistry and Physics Discussions*, *2022*, 1–33. Retrieved from https://acp.copernicus.org/preprints/acp-2022-314/ doi: 10.5194/acp-2022-314

Pitter, R. L., & Pruppacher, H. R. (1973). A wind tunnel investigation of freezing of small water drops falling at terminal velocity in air. *Quarterly Journal of the Royal Meteorological Society*, *99*(421), 540-550. Retrieved from https://rmets.onlinelibrary.wiley.com/doi/abs/10.1002/qj.49709942111 doi:

https://doi.org/10.1002/qj.49709942111

Pruppacher, H., & Klett, J. (2010). Microphysics of clouds and precipitation. In *Microphysics of clouds and precipitation.* Springer. doi: 10.1007/978-0-306-48100-0

Ramelli, F., Beck, A., Henneberger, J., & Lohmann, U. (2020). Using a holographic imager on a tethered balloon system for microphysical observations of boundary layer clouds. *Atmospheric Measurement Techniques*, *13*(2), 925–939. Retrieved from `https://amt.copernicus.org/articles/13/925/2020/` doi: 10.5194/amt-13-925-2020

Takahashi, T., Endoh, T., Wakahama, G., & Fukuta, N. (1991). Vapor diffusional growth of free-falling snow crystals between -3 and -23 °c. *Journal of the Meteorological Society of Japan. Ser. II*, *69*(1), 15-30. doi: 10.2151/jmsj1965.69.1_15

Takahashi, T., Nagao, Y., & Kushiyama, Y. (1995). Possible high ice particle production during graupel–graupel collisions. *Journal of the Atmospheric Sciences*, *52*(24), 4523-4527. doi: 10.1175/1520-0469(1995)052⟨4523:PHIPPD⟩2.0.CO;2

Touloupas, G., Lauber, A., Henneberger, J., Beck, A., & Lucchi, A. (2020). A convolutional neural network for classifying cloud particles recorded by imaging probes. *Atmospheric Measurement Techniques*, *13*(5), 2219–2239. Retrieved from `https://amt.copernicus.org/articles/13/2219/2020/` doi: 10.5194/amt-13-2219-2020

Uyeda, H., & Kikuchi, K. (1978). Freezing experiment of supercooled water droplets frozen by using single crystal ice. *Journal of the Meteorological Society of Japan. Ser. II*, *56*(1), 43-51. doi: 10.2151/jmsj1965.56.1_43

Waitz, F., Schnaiter, M., Leisner, T., & Järvinen, E. (2022). In situ observation of riming in mixed-phase clouds using the phips probe. *Atmospheric Chemistry and Physics*, *22*(11), 7087–7103. Retrieved from `https://acp.copernicus.org/articles/22/7087/2022/` doi: 10.5194/acp-22-7087-2022

Wendisch, M., Macke, A., Ehrlich, A., Lüpkes, C., Mech, M., Chechin, D., ... Zeppenfeld, S. (2019). The Arctic Cloud Puzzle: Using ACLOUD/PASCAL Multiplatform Observations to Unravel the Role of Clouds and Aerosol Particles in Arctic Amplification. *Bulletin of the American Meteorological Society*,

100(5), 841-871. doi: 10.1175/BAMS-D-18-0072.1

Wyser, K. (1999). Ice crystal habits and solar radiation. *Tellus A: Dynamic Meteorology and Oceanography*, *51*(5), 937-950. Retrieved from `https://doi.org/10.3402/tellusa.v51i5.14503` doi: 10.3402/tellusa.v51i5.14503

Yi, B., Yang, P., Baum, B. A., L'Ecuyer, T., Oreopoulos, L., Mlawer, E. J., ... Liou, K.-N. (2013). Influence of ice particle surface roughening on the global cloud radiative effect. *Journal of the Atmospheric Sciences*, *70*(9), 2794 - 2807. Retrieved from `https://journals.ametsoc.org/view/journals/atsc/70/9/jas-d-13-020.1.xml` doi: 10.1175/JAS-D-13-020.1

Young, G., Jones, H. M., Choularton, T. W., Crosier, J., Bower, K. N., Gallagher, M. W., ... Flynn, M. J. (2016). Observed microphysical changes in Arctic mixed-phase clouds when transitioning from sea ice to open ocean. *Atmospheric Chemistry and Physics*, *16*(21), 13945–13967. doi: 10.5194/acp-16-13945-2016